THE JOURNAL OF PHYSICAL CHEMISTRY B LETTERS

**2005,** *109,* 18211−18213
Published on Web 09/14/2005



# Ab Initio Surface Phase Diagram of the {10$\bar{1}$4} Calcite Surface

**Sebastien Kerisit, Arnaud Marmier, and Stephen C. Parker***

*Department of Chemistry, University of Bath, Claverton Down, Bath BA2 7AY, U.K.*

*Received: June 27, 2005; In Final Form: August 5, 2005*

Electronic structure calculations, performed at the density functional theory level, were employed to study the surface termination of the {10$\bar{1}$4} calcite surface in contact with a gaseous phase containing water and carbon dioxide. A surface phase diagram was generated to investigate the change in surface termination as a function of temperature, pressure, and gas-phase composition. This diagram revealed that a nonstoichiometric termination could occur in atmospheric conditions at high relative humidity, hence suggesting that nonstoichiometric surfaces can play a major role in the chemistry of calcite surfaces.

Calcite is a mineral of great interest to many fields of chemistry because of its presence in both geological and biological systems. The {10$\bar{1}$4} surface largely dominates the calcite morphology, and thus, its atomic structure has been the focus of numerous studies.[1−4] Many research groups,[1−4] including us,[5,6] have often regarded the stoichiometric surface as the dominant termination. In this letter, a thermodynamic formalism, used by other research groups[7−12] to study the surfaces of oxide minerals in contact with a vapor phase, is adapted to consider carbonate surfaces and thus investigate whether nonstoichiometric terminations can play a role in the chemistry of the {10$\bar{1}$4} calcite surface.

Let us consider a calcite slab in equilibrium with an atmosphere of gaseous water and carbon dioxide at temperature $T$. The mineral slab can be decomposed into $N_{CaO}$ calcium oxide units at chemical potential $\mu_{CaO}$, $N_{CO_2}$ carbon dioxide units at chemical potential $\mu_{CO_2}$, and $N_{H_2O}$ water molecules at chemical potential $\mu_{H_2O}$. The surface energy can therefore be written as

$$\gamma_{calcite} = \frac{1}{2S}(G^{SLAB}_{calcite} - N_{CaO}\mu_{CaO} - N_{CO_2}\mu_{CO_2} - N_{H_2O}\mu_{H_2O}) \quad (1)$$

where $S$ is the surface area and $G^{SLAB}_{calcite}$ is the Gibbs free energy of the calcite slab. The excess in carbon dioxide is defined by

$$\Gamma_{CO_2} = \frac{1}{2S}(N_{CO_2} - N_{CaO}) \quad (2)$$

Similarly, the excess in water vapor is defined as

$$\Gamma_{H_2O} = \frac{1}{2S} N_{H_2O} \quad (3)$$

Combining eq 1 with eqs 2 and 3 gives

$$\gamma_{calcite} = \frac{1}{2S}[G^{SLAB}_{calcite} - N_{CaO}(\mu_{CaO} + \mu_{CO_2})] - \Gamma_{CO_2}\mu_{CO_2} - \Gamma_{H_2O}\mu_{H_2O} \quad (4)$$

As the slab is in equilibrium with its bulk, the chemical potentials of CaO and $CO_2$ are not independent, i.e.,

$$g_{CaCO_3} = \mu_{CaO} + \mu_{CO_2} \quad (5)$$

where $g_{CaCO_3}$ is the Gibbs energy per $CaCO_3$ units

$$g_{CaCO_3} = \frac{G^{BULK}_{CaCO_3}}{N_{CaCO_3}} \quad (6)$$

In addition, if one assumes that the entropic contributions to the slab and bulk free energies are negligible, then eq 4 becomes

$$\gamma_{calcite} = \frac{1}{2S}(E^{SLAB}_{calcite} - N_{CaO}e_{CaCO_3}) - \Gamma_{CO_2}\mu_{CO_2} - \Gamma_{H_2O}\mu_{H_2O} \quad (7)$$

where $E^{SLAB}_{calcite}$ is the energy of the slab and $e_{CaCO_3}$ the energy of one $CaCO_3$ bulk unit, which can be both obtained from electronic structure calculations.

The computer code VASP,[13−16] a plane wave density functional theory package, was used to calculate the total energy of the systems of interest. The calculations were performed within the generalized-gradient approximation, using the exchange-correlation potential developed by Perdew et al.[17] and ultrasoft "Vanderbilt" pseudopotentials.[18,19] Preliminary tests were performed on a calcite slab in a vacuum to determine the optimal plane wave energy cutoff, $k$ point mesh, thickness of the slab, and size of the vacuum gap that maximize computational efficienty for a given accuracy. The surface area was kept constant at 5.06 × 8.14 Å$^2$. A plane wave energy cutoff of 300 eV and a 2 × 2 × 1 $k$ point mesh were found to be sufficient and thus were employed throughout this work (see Table 1). In addition, as reported in Table 2, we found that a slab consisting of five layers of 2 $CaCO_3$ units (i.e., 12.2 Å thick) was sufficient. The size of the vacuum gap had a very small effect on the surface energy, as shown in Table 3, and a gap of 18 Å was thus deemed adequate.

The self-energies of water and carbon dioxide were obtained from energy minimization of one molecule in a cubic box. The use of such calculations for gas-phase species is clearly an approximation. Thus, we adjusted the energies to better repro-

* Corresponding author. E-mail: s.c.parker@bath.ac.uk.

10.1021/jp053489x CCC: $30.25 

**TABLE 1: Surface Energy of the Dry Calcite Slab (J/m²) as a Function of the Plane Wave Energy Cutoff and *k* Point Mesh Size**

| | plane wave energy cutoff | | |
|---|---|---|---|
| *k* point mesh | 300 eV | 500 eV | 600 eV |
| 1 × 1 × 1 | −0.20 | −0.15 | −0.14 |
| 2 × 2 × 1 | 0.39 | 0.41 | 0.42 |
| 3 × 3 × 1 | 0.39 | 0.41 | 0.42 |

**TABLE 2: Surface Energy of the Dry Calcite Slab as a Function of Slab Thickness**

| layers | 1 | 2 | 3 | 5 | 8 |
|---|---|---|---|---|---|
| thickness (Å) | 0.0 | 3.05 | 6.1 | 12.2 | 21.4 |
| surface energy (J/m²) | 0.48 | 0.40 | 0.40 | 0.39 | 0.38 |

**TABLE 3: Surface Energy of the Dry Calcite Slab as a Function of the Vacuum Gap Size**

| gap size (Å) | 4 | 8 | 18 | 28 |
|---|---|---|---|---|
| surface energy (J/m²) | 0.41 | 0.39 | 0.39 | 0.39 |

duce the experimental chemical potentials of gaseous species from the reaction with CaO. In the case of water, a correction was not necessary, while the chemical potential of carbon dioxide was adjusted to reproduce the experimental enthalpy of the following reaction:

$$CaO(s) + CO_2(g) \rightarrow CaCO_3(s)$$

The change in chemical potential due to the temperature is accounted for by the following formula (shown for $H_2O$ but also valid for $CO_2$):

$$\mu^0_{H_2O}(T) = \mu^0_{H_2O}(T^0) + T^0 \cdot s_{H_2O}(T^0) + \Delta h_{H_2O}(T^0, T) - T \cdot s_{H_2O}(T) \quad (8)$$

where $s_{H_2O}$ and $\Delta h_{H_2O}$ are taken from experimental tabulated data.[20] If it is assumed that water and carbon dioxide behave as ideal gases, then the effect of the gas partial pressure on its chemical potential is given by (again, only shown for $H_2O$)

$$\mu_{H_2O}(T) = \mu^0_{H_2O}(T) + \frac{1}{2} k_B T \log\left(\frac{\rho_{H_2O}}{\rho^0}\right) \quad (9)$$

Hence, the surface energy of a particular termination can be calculated for any temperature and vapor-phase composition. If an extensive survey of surface terminations is undertaken for the surface of interest, then a phase diagram, showing the change in surface composition as a function of water and carbon dioxide, can be drawn.

An energy minimization of the stoichiometric surface was performed in dry conditions and with a monolayer of water adsorbed on the surface. Both associative and dissociative water adsorptions were considered. In the latter case, a hydroxyl group was positioned above each surface calcium atom and a hydrogen atom above an oxygen atom. On minimization, the hydrogen atom moved from the surface oxygen to bond directly to the hydroxyl group oxygen atom, thereby reforming a water molecule. This calculation suggests that dissociatively adsorbed water on calcite is energetically unfavorable, and hence, only molecular water was adsorbed on all the surfaces. Two types of nonstoichiometric surfaces were also considered:

(i) Type I surfaces (noted $R_1$ in the surface phase diagram): whereby 50% or 100% of the surface carbonate groups were removed and two hydroxyl groups were adsorbed on the surface for each carbonate group removed. This was to account for the possible reaction of the surface with water to give carbon dioxide

$$nCaCO_3(s) + H_2O(g) \rightarrow Ca_n(CO_3)_{(n-1)}(OH)_2(s) + CO_2(g)$$

This reaction results in a carbonate-poor surface.

(ii) Type II surfaces (noted $R_2$ in the surface phase diagram): whereby 50% or 100% of the surface calcium atoms were removed and two hydrogen atoms were added to carbonate groups on the surface for each calcium removed. This was to account for the possible reaction of the surface with water and carbon dioxide

$$nCaCO_3(s) + H_2O(g) + CO_2(g) \rightarrow Ca_n(CO_3)_{(n+1)}H_2(s)$$

This reaction results in a calcium-poor surface.

Both types of nonstoichiometric surfaces were considered dry and with a monolayer of water adsorbed. This leads to ten possible terminations for the $\{10\bar{1}4\}$ surface, which has two surface calcium atoms and carbonate groups (namely, stoichiometric, type I 50% and 100% reacted, type II 50% and 100% reacted. Each can be either dry or hydrated). One to three energy minimizations were carried out for each possible termination.

The surface phase diagram is shown in Figure 1. The white and shaded areas display the ranges of water and carbon dioxide chemical potentials for which a particular termination is the most stable surface of all of those considered in this work. The *x* and *y* axes show the change in chemical potential with respect to the chemical potential at 0 K. To relate the chemical potentials to more explicit physical conditions, we added vertical and horizontal lines which represent the gases chemical potential at different temperatures for a partial pressure of 1 bar (i.e.,

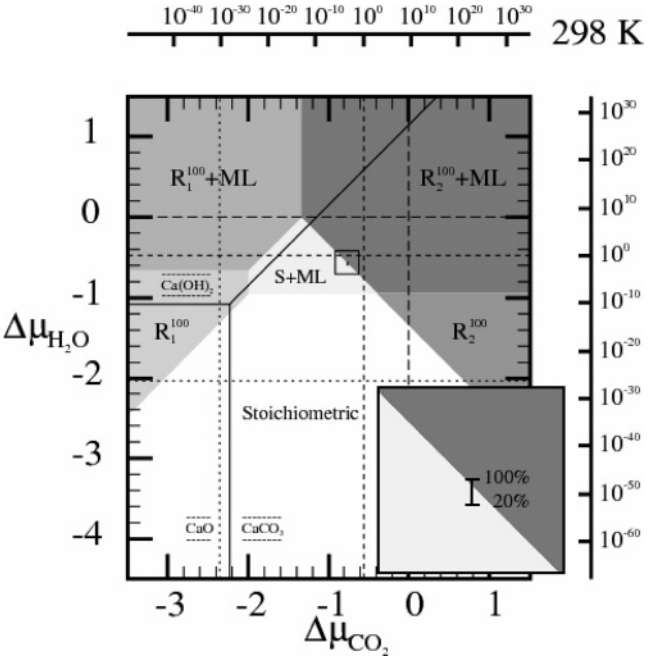


**Figure 1.** $\{10\bar{1}4\}$ Surface phase diagram, where S stands for stoichiometric and ML for monolayer. Chemical potentials and partial pressures are expressed in eV and bar, respectively. The white and shaded areas show the region in which a particular termination has the lowest surface energy. The solid lines separate the regions of thermodynamic stability of the three possible solid phases, namely, CaO, $Ca(OH)_2$, and $CaCO_3$. The long-dashed lines refer to the chemical potentials at 0 K and $CO_2$ and $H_2O$ activities of 1, while the short-dashed and dotted lines refer to unit activities at 298 and 1000 K, respectively. The inset identifies the position in the phase diagram of partial pressures of $H_2O$ and $CO_2$ found under ambient conditions and shows the effect of the relative humidity on the surface termination.

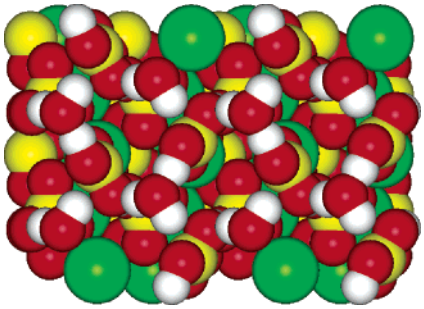

**Figure 2.** Top view of the calcium-poor hydrated $\{10\bar{1}4\}$ calcite surface. Calcium atoms are green, carbon yellow, oxygen red, and hydrogen white.

long-dashed lines, 0 K; short-dashed lines, 298 K; dotted lines, 1000 K). In addition, two extra scales were added to show the effect of partial pressure (in bar) on the gases chemical potential at 298 K. Finally, there is an equilibrium among CaO, $Ca(OH)_2$, and $CaCO_3$ that depends on the water and carbon dioxide chemical potentials. The solid lines show the boundaries between each solid phase.

The surprising feature of the phase diagram is that the boundary between the hydrated stoichiometric and calcium-poor terminations is very near to the area corresponding to atmospheric conditions (roughly the area inside the square). The inset in Figure 1 shows that the hydrated calcium-poor surface (noted $R_2^{100}$ + ML) is predicted to be the most stable termination at high relative humidity (where $\rho_{H_2O} = 0.04$ bar was taken as 100% humidity). This surface is terminated by a layer of carbonic acid groups, as shown in Figure 2. The hydrogen atoms of the carbonic acid groups form very short hydrogen bonds with the carbonate groups from the layer below (1.44 Å). All the water molecules adsorbed on the surface are equivalent, and each accepts a hydrogen bond from a carbonic acid group. These hydrogen bonds are also very short (1.37 Å). Each water molecule also forms two hydrogen bonds with two surface oxygen atoms (1.70 and 2.18 Å). It is worth noting that the symmetry of the surface is unchanged by this reaction.

Another feature of the $\{10\bar{1}4\}$ surface phase diagram is that none of the 50% reacted terminations appear in the phase diagram. Larger surface areas would be required to test the stability of surfaces where only a small percentage of the surface has reacted. However, this is beyond our present computer capabilities. The dry stoichiometric and calcium-poor surfaces can be obtained at high temperatures (about 500 K) or at very low partial pressure of water (lower than $10^{-10}$ bar), which are relevant to ultrahigh-vacuum experiments. The carbonate-poor surfaces, whether dry or hydrated, are not thermodynamically stable, as the diagram predicts that in these conditions calcite would transform to calcium oxide or calcium hydroxide, depending on the water chemical potential.

In conclusion, these calculations suggest that nonstoichiometric surfaces may be of significant importance when considering the atomic structure of calcite surfaces. Moreover, as the $\{10\bar{1}4\}$ surface is the most stable surface, it should display the smallest effect of all calcite surfaces. Thus, considering other surfaces may show a more dramatic effect. In the future, it would be very interesting to extend the thermodynamically formalism described in this work to mineral surfaces in contact with a liquid phase. Although molecular dynamics calculations would probably be required to treat such systems, continual advances in computer power could make these calculations feasible soon.

**Acknowledgment.** The authors thanks Dr. D. Cooke for useful discussions and EPSRC grant GR/H0185 for financial support.

## References and Notes

(1) Fenter, P.; Geissbuhler, P.; DiMasi, E.; Srajer, G.; Sorensen, L. B.; Sturchio, N. C. *Geochim. Cosmochim. Acta* **2000**, *64*, 1221−1228.
(2) Liang, Y.; Lea, A. S.; Baer, D. R.; Engelhard, M. H. *Surf. Sci.* **1996**, *351*, 172−182.
(3) Rachlin, A. L.; Henderson, G. S.; Goh, M. C. *Am. Miner.* **1992**, *77*, 904−910.
(4) Geissbuhler, P.; Fenter, P.; DiMasi, E.; Srajer, G.; Sorensen, L. B.; Sturchio, N. C. *Surf. Sci.* **2004**, *573*, 191−203.
(5) de Leeuw, N. H.; Parker, S. C. *J. Phys. Chem. B* **1998**, *102*, 2914−2922.
(6) Kerisit, S.; Parker, S. C.; Harding, J. H. *J. Phys. Chem. B* **2003**, *107*, 7676−7682.
(7) Wang, X. G.; Weiss, W.; Shaikhutdinov, S. K.; Ritter, M.; Petersen, M.; Wagner, F.; Schlogl, R.; Scheffler, M. *Phys. Rev. Lett.* **1998**, *81*, 1038−1041.
(8) Wang, X. G.; Chaka, A.; Scheffler, M. *Phys. Rev. Lett.* **2000**, *84*, 3650−3653.
(9) Reuter, K.; Stampfl, C.; Scheffler, M. In *Handbook of Materials Modeling*; Yip, S., Ed.; Springer: Dordrecht, 2005; Vol. 1.
(10) Batyrev, I.; Alavi, A.; Finnis, M. W. *Faraday Discuss.* **1999**, 33−43.
(11) Batyrev, I. G.; Alavi, A.; Finnis, M. W. *Phys. Rev. B* **2000**, *62*, 4698−4706.
(12) Marmier, A.; Parker, S. C. *Phys. Rev. B* **2004**, *69*, 115409.
(13) Kresse, G.; Hafner, J. *Phys. Rev. B* **1993**, *47*, 558−561.
(14) Kresse, G.; Hafner, J. *Phys. Rev. B* **1994**, *49*, 14251−14269.
(15) Kresse, G.; Furthmuller, J. *Phys. Rev. B* **1996**, *54*, 11169−11186.
(16) Kresse, G.; Furthmuller, J. *Comput. Mater. Sci.* **1996**, *6*, 15−50.
(17) Perdew, J. P.; Chevary, J. A.; Vosko, S. H.; Jackson, K. A.; Pederson, M. R.; Singh, D. J.; Fiolhais, C. *Phys. Rev. B* **1992**, *46*, 6671−6687.
(18) Vanderbilt, D. *Phys. Rev. B* **1990**, *41*, 7892−7895.
(19) Kresse, G.; Hafner, J. *J. Phys.: Condens. Matter* **1994**, *6*, 8245−8257.
(20) *CRC Handbook of Chemistry and Physics*; CRC Press: Boca Raton, FL, 1981.